5-2021

Vertical Transmission of Zika Virus in an Opossum Model

Dionn Carlo Silva
The University of Texas Rio Grande Valley

VERTICAL TRANSMISSION OF ZIKA VIRUS IN AN OPOSSUM MODEL

A Thesis

by

DIONN CARLO SILVA

Submitted to the Graduate College of
The University of Texas Rio Grande Valley
In partial fulfillment of the requirements for the degree of

MASTER OF SCIENCE

May 2021

Major Subject: Molecular Biology and Biochemistry

VERTICAL TRANSMISSION OF ZIKA VIRUS IN AN OPOSSUM MODEL

A Thesis
by
DIONN CARLO SILVA

COMMITTEE MEMBERS

Dr. John M. Thomas III
Chair of Committee

Dr. Robert Dearth
Committee Member

Dr. John VandeBerg
Committee Member

Dr. Matthew Terry
Committee Member

May 2021

ABSTRACT

Silva, Dionn Carlo A., Vertical Transmission of ZIKV in an opossum model. Master of Science (MS), May 2021, 43 pp., 5 tables, 6 figures, 69 references, 22 titles.

This study will identify Brazilian ZIKV infection in the offsprings of mated, inoculated *Monodelphis domestica* females. Unlike non-human primates (NHP) and transgenic mice, *M. domestica* provides an opportunity to study ZIKV infection in a novel animal model possibly useful for in-utero studies. *M. domestica* has also been used in cancer and dietary research with varying degrees of success. ZIKV infection will be identified using antibody staining and in situ hybridization. The expected result of this study is that ZIKV will be identified in various tissues and reveal that ZIKV is transmitted vertically in this animal model. The significance of this study is by identifying ZIKV infection and confirming vertical transmission in *M. domestica*, this will lay a foundation for future in-utero studies with this animal model.

DEDICATION

This thesis is dedicated to my father, Dionisio V. Silva, and my mother, Liza A. Silva. Thank you for being supportive throughout my undergraduate and graduate career.

ACKNOWLEDGEMENTS

I would like to acknowledge my mentor and chair, Dr. John Thomas III, for his guidance and humor as I complete my Masters'. Thank you for assisting me throughout my project. I am grateful to be in your lab as I've learned so many things over the past two years.

I would also like to acknowledge Dr. John VandeBerg and his team led by Susan Mahaney, for not only providing, handling, and processing the opossums in these experiments, but for also providing guidance and help any way they could. In addition, I would like to thank Dr. Robert Dearth and Dr. Matthew Terry for their assistance not only in the immunohistochemistry, but also in their knowledge of tissue preservation and tissue staining.

Finally, I would like to thank the lab members for their help in processing some samples: Oscar Quintanilla, Juan Garcia Jr., Jonathan Kasofsky, Eli Ruiz, Kevin Gongora, and Bridger Southwell. In addition, I would like to thank Nathan Garza for his assistance in the analysis. Lastly, thank you to Laura being helpful along the way.

TABLE OF CONTENTS

Page

LIST OF TABLES

Page

LIST OF FIGURES

Page

CHAPTER I

INTRODUCTION

1.1 Overview of this Chapter

This chapter will describe Zika virus and discuss the various vertical transmission studies done on ZIKV-infected animals. This chapter will also introduce *Monodelphis domestica*, as a possible novel animal model for ZIKV pathogenesis studies.

1.2 Zika Virus

Zika virus (ZIKV) is a flavivirus that originates from the Ziika forest in Uganda, where the virus was isolated from a rhesus monkey in 1947 (Dick et al., 1952). ZIKV is positive-sense single-stranded RNA that contains three structural and seven non-structural proteins. ZIKV has a single open reading frame (ORF) flanked by a 5' and 3' untranslated region. The ORF is what encodes the polyprotein to yield the three structural and seven nonstructural proteins. One of these proteins, the envelope (E) protein, is responsible for targeting virus to host cell receptor interactions and functions as a mediator in allowing viral entry into the cell (Kuhn, 2015). Similar to other flaviviruses such as dengue and yellow fever, ZIKV is transmitted through infected female mosquitoes, such as the Ae. aegypti and Ae. albopictus species. Both Ae. aegypti and Ae. albopictus have high vectoral capability for ZIKV, meaning that the efficacy of transmitting ZIKV in these species increases based on several factors such as number of bites and population density of female mosquitoes (Rather et al., 2017). In addition to transmission by

infected female mosquitoes, various studies have shown vertical transmission of the virus from mother to offspring.

1.3 Vertical Transmission of ZIKV

Early ZIKV studies of the possibility of vertical transmission showed the presence of viral particles and RNA in the amniotic fluid of the fetus, as well as ZIKV viral antigens being present in the placenta and miscarriage tissues of infected mothers (Calvet et al., 2016; Meaney-Delman et al., 2016). More recent studies reported how routes of perinatal transmission are mainly transplacental and how primary human endometrial stromal cells are able to support ZIKV replication (Colt et al., 2017; Pagani et al., 2017). Lastly, a recent study about ZIKV replication in prostate cells may lead to the explanation on how ZIKV is sexually transmitted. That study described how ZIKV can infect human prostate stromal mesenchymal stem cells as well as epithelial cells and lead to their replication in the human prostate, perhaps a potential source of the sexually transmitted disease (Spencer et al., 2017). These studies illustrated various transmissions of ZIKV and how ZIKV is present in the developing fetus. The importance of the effects of viral replication on the developing fetus have been previously studied in humans, NHPs, and mice. Animal models such as transgenic mice and non-human primates (NHPs) used in ZIKV research do display many limitations, such as a lack of an intact immune system as well as long developmental times. Here, we introduce an opossum model, *Monodelphis domestica*, as a novel model for ZIKV pathogenesis. At birth, *M. domestica* pups are developmentally equivalent to a 5-week-old human and they are beginning to develop an immune response. This makes the pups a unique extrauterine model in terms of early developmental animals.

1.4 Problem Statement

Studying ZIKV infection from an early developmental period and its possible vertical transmission has its difficulties not only in NHPs, but also in transgenic mice. Here, a novel marsupial model, *M. domestica*, was introduced in order to study the disease progression of ZIKV in newborn pups from ZIKV-infected dams.

1.5 Research Objective

The purpose of this study addresses three key points. The first was to confirm vertical transmission from the dams to the pups at various age points: 0-days, 3-days, 6-days, 9-days, and 12-days. The second was to determine the frequency of infection of ZIKV in newborn pups, as at birth, newborn pups are developmentally equivalent to a 5-week-old human. Lastly, this animal model will be evaluated to determine if *M. domestica* can be a viable model for future in-utero studies.

Based on initial studies with this model, it is expected that the pups be susceptible to vertical transmission. However, varying amounts of anti-NS1 antibody detected may vary depending on the age of these newborn pups. Antibody staining was used to confirm ZIKV-infection of these newborn pups and infection rates based on tissues analyzed and infection rate was determined.

CHAPTER II

REVIEW OF THE LITERATURE

2.1 Overview of this Chapter

This section reviews information about ZIKV vital to understanding the purpose of studying ZIKV pathogenesis in a novel opossum model. The importance of the laboratory opossum, M. domestica, will be discussed as well as its purpose in this study.

2.2 Viral Structure and Genomics

Research concerning the ZIKV genome illustrated two principal viral lineages originating from Asia and Africa. Phylogenic analysis using nucleotide sequences of 29 ZIKV genomes revealed that strains like PRVABC-59 is an Asian lineage-derived American strain (Yun et al., 2016).

The ZIKV particle is spherical in nature, approximately 50nm in diameter, and encompasses three structural proteins: the capsid (C), the pre-membrane/membrane (prM/M), and the envelope (E) (Suchetana et al., 2005). The capsid plays an important role in flavivirus assembly. Similar to other flaviviruses, ZIKV E protein contains four domains. Both the E and M glycoproteins are located at the lipid bilayer, which allows for the formation of heterodimers due to their transmembrane domains leading to the rise of the viral particle's outer surface (Yun and Lee, 2017). Other than the 3 structural proteins, ZIKV also has 7 structural proteins. Unlike the structural proteins that aim to form the viral particle, the nonstructural proteins function in genome packing as well as assisting in viral replication (Sirohi et al., 2017).

When compared to other flaviviruses, however, ZIKV structure illustrates a common

organization apart for some minor differences (Sirohi et al., 2017). One example can be seen in viral E proteins of Dengue virus (DENV) being almost structurally similar to that of ZIKV. Another example is in the organization of the protein in flaviviruses being very similar but not entirely identical to that of ZIKV. In many flaviviruses, the NS1 protein is associated with the viral replication complex on the ER, which can exit cells to form hexamers, and can even bind to uninfected cells via glycosaminoglycan interactions (Avirutnan et al., 2007).

Another important protein for viral replication in ZIKV is nonstructural protein 5 (NS5). The NS5 protein in ZIKV consists of two domains: a RNA-dependent RNA polymerase (RdRp) domain at the C- terminal and a methyltransferase (MTase) domain at the N-terminal (Elshahawi et al., 2019). In DENV, RdRp and MTase domains interact and increase RNA replication efficiency. First, the primers would be synthesized complimentary to the 3' end followed by conformational changes which elongate the RNA. Following research depicted the importance of the MTase domain at increasing efficiency of initiation, priming, and elongation steps and was found to be the same in ZIKV (Potisopon et al., 2014; Zhao et al., 2017). In addition, research has shown that ZIKV NS5 protein shares many structural similarities to that of Japanese encephalitis virus (JEV) due to how conserved the loops and beta sheets are in the MTase domain (Zhao et al., 2010).

2.3 Transmission Cycle and Viral Replication

ZIKV can persist in two transmission cycles. The first is an enzootic cycle that includes primates and primarily the Aedes genus of mosquitos. Some species, such as the Aedes albopictus has a high potential of circulating the virus in this cycle (Bueno et al., 2016). The other is an urban cycle in which transmission of ZIKV is from humans to urban mosquitoes (Weaver et al., 2016). Mosquitoes will acquire the virus through a blood meal, host it in their

bodies throughout their lifetime, and can transmit the virus through the bite of infected Aedes species, such as A. aegypti and A. albopictus (Zhao et al., 2018). Other possible routes of transmission can include perinatal transmission from mother to fetus, blood transfusions, and sexual activities (Musso et al., 2014).

When an infected female mosquito feeds on the host, viral particles will be released to the bloodstream which then infect various cells. Because ZIKV is a flavivirus, the viral particles will enter through specific receptors or clathrin-coated vesicles of the cell membrane. ZIKV does this by attaching the E protein to host receptors and allowing it to enter the host cell through apoptotic mimicry. Following this, the virus membrane then fuses with the host endosome. Following membrane fusion, E trimers are formed due to acidic pH triggers that lead to the release of the nucleocapid into the cytoplasm (Rodriguez et al., 2019). In the cytoplasm, the single stranded RNA will be translated into a polyprotein, then cleaved into the 3 structural and 7 nonstructural proteins. The viral genome will then be replicated, and viral assembly will take place on the surface of the endoplasmic reticulum. The immature viral particle will travel through the Golgi network, where the virions will mature and then be released via exocytosis (Roby et al., 2015). The virions are then able to spread throughout the body and possibly reproduce in certain immune-privileged sites. Research has shown the persistence of ZIKV in varying immune-privileged sites like the eyes and testes (Jampol and Goldstein, 2016; Venturi et al., 2014).

2.4 Neurological Effects and Complications

ZIKV has been linked to numerous neurological conditions and complications such as Guillain-Barre syndrome (GBS), meningoencephalitis, transverse myelitis (TM), and many other others. ZIKV-induced pathogenesis and the mechanisms surrounding it are still poorly

understood. However, researchers have described mechanisms in which ZIKV can avoid host IFN signaling of STAT2. When IFN-1 pathways are activated in response to viral infection, IFN-simulated response elements will be expressed. The NS5 ZIKV protein can then bind and destroy the STAT2 through proteasomal degradation, thus having resistance to IFN (Kumar et al., 2016; Grant et al., 2016). Another mechanism that may link ZIKV infection to a neurological disease can be seen in the inhibition of RIG-I molecules. These RIG-I-like receptors are viral RNA sensors that trigger an immune response through type I IFN production (Oshiumi et al., 2016). Therefore, defects in these defense mechanisms may facilitate GBS manifestation when infected with ZIKV. Research has also shown ZIKV infection triggering cytopathic effects in infected cells, which leads to morphological changes in the cell and eventually implosive cell death (Monel et al., 2017). In addition, any failure in the expression of the IFN induced transmembrane family proteins may lead to an increase in ZIKV-induced cell death (Savidis et al., 2016).

In terms of ZIKV proteins, a recent study suggests that cell-cycle disturbances, inhibition of cell proliferation, and cell death are due to ZIKV protein expression. Expression of proteins such as the M protein, E protein, and NS4A lead to cells accumulating in the G2/M phase, while expression of the prM protein results in cells accumulating in the G1 phase (Li et al., 2017).

Viral survival in the central nervous system (CNS) may be associated with the activation of mTOR and anti-apoptotic pathways, which may explain various neurological manifestations caused by ZIKV, even when there is viral clearance from the blood (Aid et al., 2017). GBS, for example, can be characterized as the activation of the immune response leading to damage in the peripheral nervous system (Sejvar et al., 2011). Research in ZIKV has depicted the virus to be a cause for triggering onset of GBS (Monsalve et al., 2017). Although the

molecular mechanisms for this are still not very well known, host-virus interactions focusing on humoral immunity, T-cell immunoreactivity, and molecular mimicry have been proposed to induce GBS (Munoz et al., 2016). In terms of molecular mimicry, ZIKV polyproteins do share peptides with human proteins. Research has shown that if ZIKV infection cross-reacts with these human proteins, any alterations may contribute to ZIKV-associated neurological complications such as GBS (Lucchese and Kanduc, 2016).

2.5 Current ZIKV Animal Models

Several studies in various animal models have illustrated adverse effects of viral replication in the developing fetus. The sudden declaration of ZIKV as a global health emergency in 2016 launched a campaign to establish animal models to explore transmission and pathogenesis of ZIKV. These animal models would then be used to evaluate therapies and vaccines produced. Some of these animal models include various mouse models, non-human primates (NHPs), and other atypical models.

One type of mouse model is the immunocompetent mouse, meaning the mouse has a normal immune response. In 1-day-old C57BL/6 mice that were subcutaneously inoculated with ZIKV, there was no evidence of viral infection in the spleen or liver (Manangeeswaran et al., 2016). Virgin female C57L/6 mice that were intravaginally inoculated with ZIKV showed persistence of the virus, and there was significant intrauterine growth retardation (IUGR) in the fetesus of those mice infected on E4.5 (Yockey et al., 2016). This study also showed the presence of ZIKV in the fetal brains, suggesting the sexual transmission of ZIKV in mice (Yockey et al., 2016). In addition, ZIKV has been inoculated into pregnant mice or directly into the brain of the developing fetus of wild-type (WT) mice or immunocompetent mouse (Morrison and Diamond, 2017). Results for many of the WT mice studies reveal how ZIKV

does not cause consistent infection of healthy WT mice. An explanation for this is because ZIKV must overcome type I interferon (IFN) signaling in order to multiply and cause infection in vertebrates (Cao et al., 2017). Furthermore, unlike the human STAT2 ortholog, ZIKV will not promote degradation of mouse STAT2 and does not establish sustained infection and viremia in mice (Grant et al., 2016; Kumar et al., 2016). Researchers would then go on to use immunodeficient mice such as IFNAR-deficient mice in order to show the effects of viral replication during pregnancy.

Other than immunocompetent mouse, immunocompromised mice are the main type of mouse used when studying ZIKV infection. Immunocompromised mice, such as A129 mice subcutaneously treated with ZIKV, show a reduction in weight as well as ZIKV RNA detection in various organs of the body, with the highest levels of ZIKV RNA detected in the spleen (Dowall et al., 2016). Interestingly, similar to the immunocompetent mouse, these mice showed ZIKV persisting in the sexual organs. When these pregnant A129 mice were mated with WT mice, ZIKV RNA was shown to be present in various trophoblast cells in the placenta, which are consistent with results from a cell culture study showing ZIKV can infect human trophoblast cells (Miner et al., 2016; Bayer et al., 2016). These ZIKV-infected placentas would also depict vascular injury, reduced fetal capillaries, and other abnormalities demonstrating how ZIKV is able to pass through the fetal blood barrier during pregnancy (Miner et al., 2016). In pregnant MAR1-5A3 mice, there was no fetal demise after ZIKV infection, however, the fetuses demonstrated a substantial amount of IUGR as well as other abnormalities (Miner at al., 2016). Another study using MAR1-5A3 showed how subcutaneous and intraperitoneal inoculation of the mice lead to high viremia and neuropathological changes; acute encephalitis and encephalomyelitis were also observed and may suggest the importance of type I IFN in suppressing ZIKV pathogenesis (Smith et al., 2017). AG129 mice were another type of

immunocompromised mice used. In ZIKV-infected AG129 mice, research has shown an increase in inflammatory cytokines and chemokines (Zmurko et al., 2016). These immunocompromised mice models, although valuable to understanding ZIKV pathogenesis, cannot support ZIKV infections *in vivo* as fatality in these mice models are common. Other than mouse models, NHPs are another model used to study ZIKV pathogenesis.

The importance of NHPs in ZIKV research is illustrated in their ability to exhibit clinical signs unlike in mouse models. One example of a NHP commonly used for ZIKV research is the rhesus macaques. Pregnant macaques that were infected with ZIKV showed an increase in innate and adaptive immunocytes at 6 days post infection (dpi), a decrease in total leukocyte numbers at 10 dpi, and high neutralizing antibody (nAb) titers at 14 dpi (Dudley et al., 2016). An in-utero transmission was successfully done on a pregnant pigtail macaque with Cambodian ZIKV strain corresponding to around 28 weeks of human pregnancy; these results would reveal reduced growth of the fetal brain, white matter deficiency and gliosis, and axonal damage (Adams Waldorf et al., 2016). These macaque studies and other NHP studies are important in depicting that ZIKV can pass through the fetal blood barrier, damage the fetal brain, and illustrate the impact of sexual transmission of ZIKV and its affects on the mother and fetus.

ZIKV infection has also been shown in other atypical models, more specifically the chick embryo and in cell culture. Chick embryos have many uses in developmental biology, and when infected with ZIKV, researchers found that the total brain volume decreased and the ventricular space increased. This suggests less cortical tissue in the ZIKV-infected chick embryos compared to the controls (Goodfellow et al., 2016). Other than chick embryos, various cell cultures have also been used to study ZIKV infection.

ZIKV infection in human neural progenitor cells (hNPCs) have been shown to lead to

dysregulation of various cell cycle genes and lead to apoptotic death (Tang et al., 2016). Furthermore, an organoid study on the forebrain revealed similar features to that of microcephaly in ZIKV-infected samples. The significance of that study illustrated the decrease of neuronal layer in terms of thickness and overall brain size (Qian et al., 2016).

With its unique molecular mechanisms, further research on ZIKV pathogenesis is needed. Although these animal models have their benefits, they have many limitations which include but are not limited to: costs, time of growth, and high mortality. Perhaps with these limitations, novel animal models may arise to help further understand ZIKV pathogenesis.

2.6 Advantages of the lab opossum

Monodelphis domestica, the gray short-tailed opossum, is a marsupial native to Brazil. These opossums can produce large litters, are generally docile, can breed in captivity, and have been well established as a laboratory marsupial by VandeBerg and researchers (VandeBerg 1983, 1990). These large litters and the ability to reproduce consistently allow this animal model to have the advantage of being more cost friendly as well as having a larger sample size than other traditional animal models. In addition, these species of laboratory marsupials have made great contributions to biomedical research. What is especially interesting about these opossums is that birth after a short gestation period allows for additional manipulation of opossum pups at an immature stage of development (Tyndale-Biscoe and Janssens, 1988). These neonatal pups are equivalent to a 5-week-old human embryo (Cardoso-Moreira et al., 2019). Another advantage for these female opossums is that they lack a pouch, meaning the pups will remain attached to the mother opossum for the first 14 days. These pups serve as important exteriorized fetal models, as observing ZIKV pathogenesis in ZIKV infected pups would give a better understanding of ZIKV pathogenesis in the first trimester of human

pregnancy (Caine et al., 2018). Other reasons for the use of these opossums arose in order to study their physiological systems.

Monodelphis domestica has previously been used in cancer and dietary studies, which may prove insightful when using this animal model as a candidate for ZIKV infection. One cancer study describes how researchers were able to identify dimers in DNA of *M. domestica* as a major photoproduct associated with induction of sunburn cells and hyperplasia (Ley and Applegate, 1985). Other melanoma studies would include exposing the opossums to various grade doses of ultraviolet radiation A (UVA) in which the results would show the efficacy to induce focal melanocytic hyperplasia (FMH) and nonmelanoma skin tumors (NMST) using UVA is not effective as only high doses of UVA significantly induced FMH and NMST (Ley, 2007). Skin and eye tumor studies were also conducted on this opossum model in which the results suggested dimers play a role in the induction of cutaneous tumors and photoreactivating light significantly delayed the appearance of corneal tumors (Ley, 1991). All of these cancer studies illustrate the importance and significance of this opossum model in further understanding tumor studies. Furthermore, M. domestica has also been used in several dietary studies.

One dietary study describes how genetic variation in ABCB4 genes are responsible for dramatic differences in their non-HDL cholesterol response due to an atherogenic diet (Kammerer et al., 2010). Another study illustrates the effect dietary cholesterol with or without saturated fat on plasma lipoprotein cholesterol levels, revealing that perhaps the genes for dietary response affects the response to dietary cholesterol but not to saturated fat (Kushwaha and VandeBerg, 2004). These cancer and dietary studies both show the viability of the opossum animal model, and perhaps how it can be further expanded to in utero studies.

What makes this opossum model worth studying is the similarities in immune systems

when compared to humans. Research on the cellular immune response of M. domestica reveals a significant finding: the immune response of M. domestica is similar to that of eutherian mammals except for the observation of weak MLC responses (Infante et al. 1990). With similar immune responses to that of a human, perhaps this animal model may be considered. In addition,

This study will evaluate Brazilian ZIKV infection in the offspring of mated, inoculated *M. domestica*, which has been used for diabetic research and has a similar immune response to that of a human. The analysis of ZIKV in the possum will be performed via antibody staining and confirmation tests from dissected heads and bodies.

2.7 Limitations of ZIKV Research

Although current and conventional methods of studying ZIKV pathogenesis have provided an insight on many pathways and mechanisms, there are nonetheless practical and biological limitations present. For example, studies looking at ZIKV infection from a gestational stage do not go past the 20-day post infection stage in mice models (van Den Pol et al., 2017). Many ZIKV infection studies evaluate these animal models past their immature stages, but more research is needed to understand how ZIKV pathogenesis impacts the immature animal models leading to their maturation. One mice study, however, did evaluate ZIKV infection in neonatal mice and found abnormalities in brain pathology, but did not mention about infection in other tissues (Nem de Oliveira Souza et al., 2018).

CHAPTER III

MATERIALS AND METHODS

3.1 Overview of this Chapter

This experiment will be conducted at the University of Texas Rio Grande Valley – Edinburg Campus. A colony of *Monodelphis domestica* is kept at the Brownsville campus where the organs will be dissected, harvested, fixed, and then transported to the Edinburg campus. Tissue fixation can be done in either campus.

3.2 Newborn opossums

All newborn opossum pups used in this study were produced in the breeding colony by mating infected females with non-infected males. The breeding colony is maintained at the University of Texas Rio Grande Valley and maintained under standard conditions (Vandeberg and Blangero, 2010).

3.3 Ethics Statement

All animal work described herein was subject to review and approval by the UTRGV Institutional Animal Care and Use Committee (IACUC), as well as oversight provided by the UTRGV Department of Laboratory Animal Resources (LAR). LAR maintains compliance with the National Institutes of Health Office of Laboratory Animal Welfare (NIH OLAW) Public Health Service (PHS) Policy on Humane Care and Use of Laboratory Animals; PHS Assurance number A4730-01, and the United States Department of Agriculture (USDA); USDA Assurance number 74-R-0216. The animal protocol for this work was approved and conducted under the IACUC protocol of Dr. John Thomas (#2016-005-IACUC).

3.4 Tissue Fixation

The tissues will be dissected and prepared as needed. Next, the following will be added to the tissues: 200 µl of 0.5 M egtazic acid (EGTA), 200 µl 10X Phosphate buffered saline (PBS), and 140 µl formaldehyde (37%). The tissues will be nutated at room temperature for 30 minutes to 2 hours, depending on the size of the tissue and degree of fixation. Next, the tissues will be washed three times, 5 minutes each with Embryo wash buffer or 1X PBS. Then remove half of the wash and replace with 100% methanol (MeOH), incubating at room temperature with gentle mixing for 5 minutes. The step that removes half of the wash, replaces the wash with MeOH, and incubates at room temperature for 5 minutes will be repeated a second time. Following the repeated step, the tissues will be washed once with 100% ethanol (EtOH). Finally, replace the wash with fresh 100% EtOH, label the type of tissue, date and store at -20°C.

3.5 Tissue embedding in preparation for sectioning

Before continuing with tissue imbedding for sectioning, the fixed tissue will be inspected for dehydration; if dehydrated, perform serial rehydration before continuing to tissue imbedding. Tissue organs will be equilibrated in optimal cutting temperature (OCT) compound. The organs will undergo a quick wash and a slow wash. For the quick wash, dispose of the fixing solution first and the tissue organs will be washed with 2 mL of PBtween three times quickly, disposing of the solution each time. For the slow wash, the organs will be washed with 2 mL of PBtween three times slowly, giving 10 minutes for each solution, disposing of the solution each time. Next, transfer about 30% OCT: 70% 1X PBS into organ containing tube. The tube will be transferred in a nutator (GyroMini) and will be incubated at room temperature for 60 minutes. The solution will be disposed of, and the organ will be washed quickly 3 times with PBtween. Transfer 60% OCT: 40% 1x PBS into organ containing tube. This tube will be transferred to the nutator (GyroMini) and will be incubated at room temperature for 60 min. After the 60 min, the solution will be disposed of and the tissues will be quickly washed 3 times with PBTween. Following the 3 quick washes, 100% OCT will be transferred into the organ containing tubes. The tube will be transferred in a nutator (GyroMini) and will be incubated overnight. The following day, these organs will be sliced and placed into slides using the Cryostat machine.

3.6 Cryostat Sectioning

A layer of OCT is applied to a base foundation where the tissues will lie. In the Cryostat machine, this layer of OCT will freeze and form a solid layer. The prepared tissue will be placed on top of this OTC layer. Surrounding this OTC layer is a clamp that will allow the inside of the clamp to be filled with OTC, forming an OTC layer around the tissue. From there, the tissues

will simply be sliced and placed onto slides. The slides will be properly labeled with the type of tissue, the number associated with the tissues, and the date sliced. Following tissue slicing in the cryostat, they are ready for antibody staining and in situ hybridization.

3.7 Antibody Staining

PBTween (50 mL PBS and 500 uL Tween 20) and 2% BSA PBTween will be prepared. A hydrophobic pen will be used to form a barrier around the sliced tissues in the slide. Next is the blocking step, which will take 1 hour and includes the addition of 100 uL of 2% BSA PBTween in each tissue. The primary antibody (1:500, NS1 and ENV) will be added for two hours or overnight and will be kept in a high humidity environment if done for two hours. Three quick washes and three slow washes with a ten-minute duration each will be done following the two hour or overnight incubation period. The secondary antibody (1:200, Alexa Flor 647 or 546) will be applied and will be incubated for two hours or overnight at 4°C. Three quick washes and three slow washes lasting 10 minutes will be applied. In the 2nd slow wash, a phalloidin mix will be added (2.5 phalloidin, 0.5ul Dapi, 500 uL PBTween 20). Next, 20 uL of mounting media or PBTween will be added to the slide and a slide cover will be applied. The slides will be sealed with nail polish and will be ready for confocal microscopy. Triplicates of each slice were done in order to ensure the most accurate reading of NS1 signal. Furthermore, each slide had two tissues slices, in which one would contain no primary antibody and the other would. Doing this would ensure that the NS1 signal coming from the tissue slice with primary antibody was true signal.

3.8 Confocal Microscopy

Standard microscopy techniques will be used to examine the tissues. First, the tissue will be lined up with the number on the strand of the microscope as these were the sections of

interest. The sections will be registered, Alexa Flor 488 and DAPI will be selected, and corresponding Alexa Flor will be used as a secondary. The image will appear, and then the laser strength will be changed accordingly as well as the focus. Pictures will be taken at 10x and 60x objective lenses. The repeat will be clicked to restart the image capture and once the image looks ready, the repeat will be turned off as the image will be ready to be taken. Lastly, channels will be assigned to the images and these images will be saved on the computer for future reference.

3.9 TUNEL Assay

A TUNEL assay was used to evaluate apoptosis in a Day 9 ZIKV-infected pup and a Day 9 control pup. First the slides were incubated at room temperature for three slow washes each at 5 minutes using PBS. Next, the tissues were covered with 100ul of proteinase K solution and incubated for 5 minutes at room temperature. The proteinase K solution would be removed, and another 5-minute wash of PBS was done. In order to label these tissues, PBS is then removed, and the premade wash buffer is used to cover the sections for 5 minutes. Next, another slow wash of wash buffer is done for 5 minutes. Then remove the wash buffer and cover the tissues with 50ul of the DNA labeling solution and incubate in 37□ for an hour. After the one hour wait, the DNA labeling solution is removed and 100ul of antibody solution is added and incubated at room temperature for 30 minutes. Next, the tissues will be washed with double distilled H_2O (ddH_2O) and incubated for 5 minutes at room temperature. The 7-AAD/RNase A staining buffer is then added to cover the tissues and incubated in the dark for 30 minutes at room temperature. Two slow washes for 5 minutes each with ddH_2O are performed after the 30-minute incubation period. Lastly, add a drop of antifade or Prolong Gold and add a cover slip to the respective slides.

CHAPTER IV

RESULTS

4.1 Antibody Stains

In order to determine possible Brazilian ZIKV vertical transmission in these pups, immunohistochemistry (IHC) was conducted on 0 day, 3 day, 6 day, 9 day, and 12 day old pups. The pup heads and bodies were stained separately. Heads and bodies were evaluated for ZIKV-NS1 protein using an immunofluorescent microscope. For validation experiments, ZIKV-infected pups were also stained without NS1 primary antibody and did not display signs of infection. ZIKV-infected pups that were stained with anti-NS1 antibody were able to display a punctate red pattern in various nuclei of the brain (Figure 1). As mentioned previously, triplicates for each individual head and body were stained and evaluated to ensure NS1 signal was prevalent throughout (Figure 4). Furthermore, a scoring system of the NS1 signal, ranging from 0 to 3 was created. For the scoring system, 0 means no NS1 signal, 1 means minimal signal, 2 means medium amount of signal, and 3 means a lot of signal. Confirmation of NS1 protein in the infected pups were also confirmed at various days 0, 3, 6, 9, and 12 alongside a sample with no NS1 added corresponding to each age group (Figure 2). Furthermore, a comparison of the PBS-treated and ZIKV-infected pups was also done (Figure 3). A preliminary TUNEL assay was also ran to assess the amount of apoptosis in some Day 9 samples (Figure 6).

During initial immunofluorescent microscopy, punctate red patterns of anti-NS1 antibody were found in the spinal vertebrae as well as the eyes of ZIKV-infected pups. These punctate red patterns in the eye were first seen in 12d pups. Sample P1467, a 12d pup, was the first pup seen to display ocular infection of ZIKV. Two other 12d pups, P1584 and P1569, were also found to display ocular infection. Other 12d control pups did not display this sort of ocular infection when examined. Furthermore, when investigated in the other days, no evidence of ocular infection was found. In addition, these punctate red patterns were also seen in the spinal vertebrae in one sample. Punctate red patterns were also seen in the spinal vertebrae of one 12d pup. This was first observed in the 12d pup P1504. The other 12d pups tested did not display this sort of punctate red patterns in the spinal vertebrae. When other 12d control pups were examined, they also did not display viral infection of the spinal vertebrae.

In total, 69% of tested and presumed ZIKV-infected pups displayed viral NS1 signal (Table 3). Although the punctate red patterns were not easily visible at 10x magnification, at 120x magnification, they were (Figure 1). Validations were also performed for each sample as previously stated. A percentage of infection based on the age was also done and illustrated how the 12d ZIKV-infected group had the largest percentage of observed infected at 100% while the lowest group was that of the 3d ZIKV-infected group at 0% (Table 4). This was primarily due to the day 3 tissues being from PBS mothers. A completed table of the tested pups with their corresponding litter groups is illustrated to show if there was any difference in ZIKV vertical transmission in these various litter groups (Table 5). Lastly, an evaluation of the infected mothers and infected pups were observed (Table 2).

CHAPTER V

DISCUSSION

This study evaluated the vertical transmission of ZIKV-BR in pups born from infected females and non-infected males. The selected age group of 0d, 3d, 6d, 9d, and 12d of various pups were evaluated in determining if there was any presence of viral NS1 protein in both the head and the body of the pups. Not only was vertical transmission seen in over 60% of the pups, but these pups also demonstrated the possibility for a novel animal model for ZIKV research. Furthermore, other infectious studies in animal models do not depict the impact of ZIKV from such an early embryonic and fetal developmental stage. Because of this, these opossum pups may even be useful in in-utero studies. In order to the susceptibility to infection these newborn opossums were, their heads and bodies were analyzed separately using IHC.

Of the total tissues analyzed, the presence of viral NS1 within the nuclei was found in 69% of those tissues when evaluated using IHC (Table 1). The NS1 protein is not only involved in viral replication, but it is also shared among the flaviviruses (Young et al., 2000). Through those evaluated tissues, its detection throughout various ages of the newborn pups illustrates the vertical transmission of ZIKV-BR in the laboratory opossum (Table 1; Figure 1). Non-specific binding of the NS1 antibody can also be ruled out due to the validation tests (Figure 1; Figure 2). Although vertical transmission was confirmed, the percentage of infection based on the age groups did vary. The age group with the most percentage infected at 100% was the Day 12 group, whereas the age group with the least percentage infected the Day 3 group in which the six tissues evaluated were all uninfected (Table 4). More research needs to be conducted, as well as

a larger sample size per age group, if there is any correlation between a certain age group and their percentage of infected. The results from the IHC indicate that the laboratory opossum pup was permissive to vertical transmission, viral infection, and replication of ZIKV-BR.

Some unexpected findings in the tissues analyzed were that some pups infected in their heads did not display viral infection in the bodies when observed through IHC. This may be due to how young the pups are and how the virus has not been able to circulate enough throughout the body yet. Various studies have illustrated ZIKV targeting the developing brain. One study depicted ZIKV infecting not only astrocyte and glial cells, but also infecting the brain loci and visual systems of mice (van del Pol et al., 2017). Another study showed the vertical transmission of ZIKV in offspring mice. That study revealed how ZIKV would infect the radial glial cells in the fetal brain and cause a reduction in the proliferative pool of cortical neural progenitor cells leading to developmental issues (Wu et al., 2016). Future studies for these pups could possibly be to identify if ZIKV can also infect radial glial cells and reduce cortical neural progenitor cells in *M. domestica* and compare to various animal models.

A further explanation of why there were discrepancies in various infected tissues can also be due to the tissues themselves. Prior to embedding, sectioning, and staining these tissues, the samples had been fixed in 10% formalin for roughly over a year. A study evaluating the effects of just this illustrated a decrease in the efficacy of immunohistochemical analysis after 7 weeks, in which a recovery antigen such as proteinase K was needed to reverse the cross-linking effects (Mostegl et al., 2011). While the formalin fixed pups may have been in formalin for a while, the frozen pups did not encounter the issue the formalin fixed pups may have had. Furthermore, it is important that these findings be evaluated dependent on the litters of the pups, as some litters may be more genetically susceptible than others to ZIKV infection. In addition, future work concerning prolonged fixation may be to use a recovery antigen prior to staining.

Detection for viral NS1 antibody occurred at varying degrees across the age groups (Figure 1). Interestingly, the highest NS1 antibody score of 3 was only in the heads, whereas the NS1 antibody scores in the bodies across the age groups would vary. To reiterate, more research needs to be conducted to see any correlations between the age groups and the persistence of infection in the head and bodies.

This study is unique in displaying vertical transmission of ZIKV-BR in the laboratory opossum. This study was meant to mimic the infection patterns of infants who are exposed to ZIKV due to vertical transmission. More importantly, this research highlights the ability for an opossum model to be susceptible to ZIKV vertical transmission. These pups were born to infected mothers and non-infected fathers, in which they were then harvested at Day 0, 3, 6, 9, and 12. Furthermore, this study provides insight in the early infection stages of ZIKV, especially when caused due to vertical transmission. It is important to keep in mind the progression of ZIKV in these pups as they age, as complications of ZIKV may present themselves at a later age. However, more research needs to be done in determining not only disease progression but the complications along with it. Nonetheless, the observation of vertical transmission of ZIKV in the laboratory opossum continues to show promise for this animal model for future viral replication studies and in-utero studies.

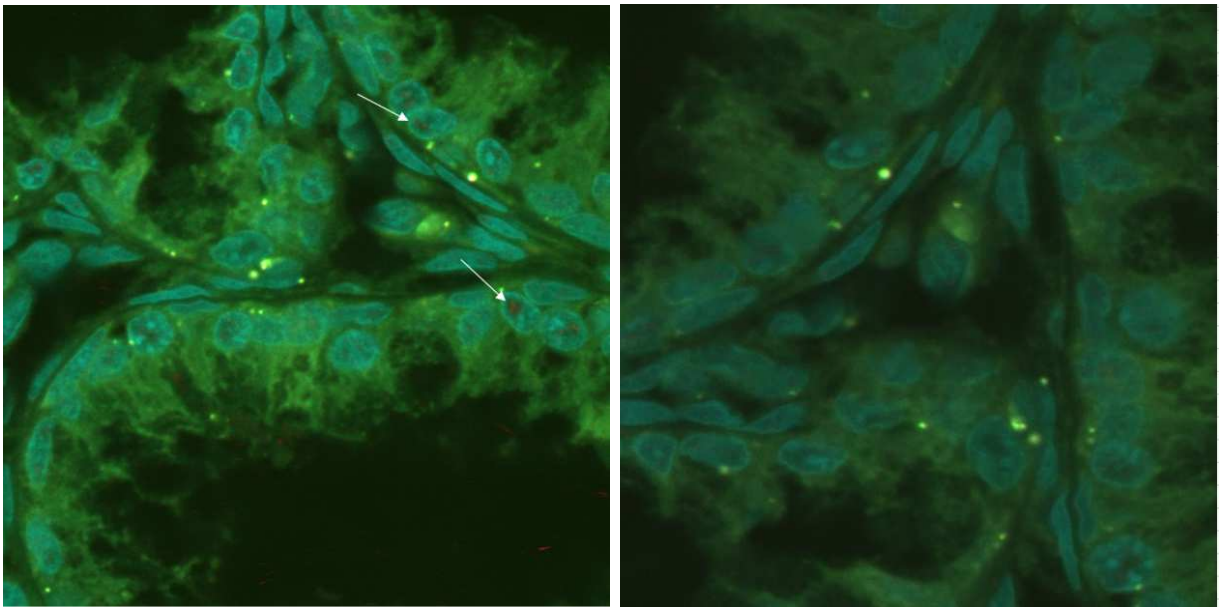

Figure 1. NS1 Antibody Validations. Figure 1A on the left shows the presence of NS1 protein through IHC when using primary antibody. Figure 1B is a similar image without primary antibody showing no presence of NS1 protein in the same tissue.

ID Number	Age (days)	Treatment	Pup Weight (g)	Tissues Analyzed		NS1 Score (Head, Body)		Additional Comments
				Head	Body	Head	Body	
P1495-12	0d	B	0.090	-	-	*	*	Formalin Fixed
P1476-9	0d	B	0.104	Y	Y	1	1	Formalin Fixed
P1494-9	0d	B	0.120	-	-	*	*	Formalin Fixed
P5078-2	0d	PBS	0.120	N	N	0	0	Frozen
P1520-11	3d	PBS	0.178	N	N	0	0	Frozen
P5077-2	3d	PBS	0.128	N	N	0	0	Formalin Fixed
P1541-9	3d	PBS	0.151	N	N	0	0	Frozen
p1569-9	6d	B	0.324	N	Y	0	1	Frozen
P1398-9	6d	B	0.256	Y	Y	1	1	Frozen
P4710-4	6d	PBS	0.462	N	N	0	0	Formalin Fixed
P1398-8	6d	B	0.166	Y	Y	0	0	Formalin Fixed
P3654-4	9d	PBS	0.408	N	N	0	0	Formalin Fixed
P1349-12	9d	B	0.549	Y	Y	1	1	Frozen
P1364-11	9d	B	0.409	Y	Y	3	1	Frozen
P1495-10	9d	B	0.367	N	-	0	*	Frozen
P1359-9	9d	B	0.399	N	-	0	*	Frozen
P1349-11	9d	B	0.502	-	Y	*	1	Formalin Fixed
P1467-10	12d	B	0.693	Y	Y	1	1	Formalin Fixed
P1495-8	12d	B	0.653	Y	-	3	*	Formalin Fixed
P1467-9	12d	B	0.726	Y	Y	1	1	Frozen
P1584-8	12d	B	0.803	Y	-	2	*	Formalin Fixed
P1591-10	12d	B	0.613	Y	Y	2	1	Formalin Fixed
P1455-9	12d	B	0.826	Y	-	1	*	Formalin Fixed
P2735-5	12d	PBS	0.639	N	N	0	0	Formalin Fixed
P1504-8	12d	PBS	0.841	-	Y	*	2	Frozen

Table 1. Detection of ZIKV-NS1 Viral Protein in Day 0, 3, 6, 9, and 12 Pups. Presence of NS1 protein indicated by the observation of secondary antibody AlexaFluor 546 (Thermo Fisher Scientific, USA). B: Brazilian Zika Virus; PBS: Phosphate buffer solution; Y: Yes- immunofluorescent signal was detected; N: No- immunofluorescent signal was not detected; *: tissues were embedded and sectioned, but not stained due to insufficient time. Presence of NS1 protein was also scored from 0 – 3, in which 0 had no observed presence of NS1 through IHC and 3 had a lot.

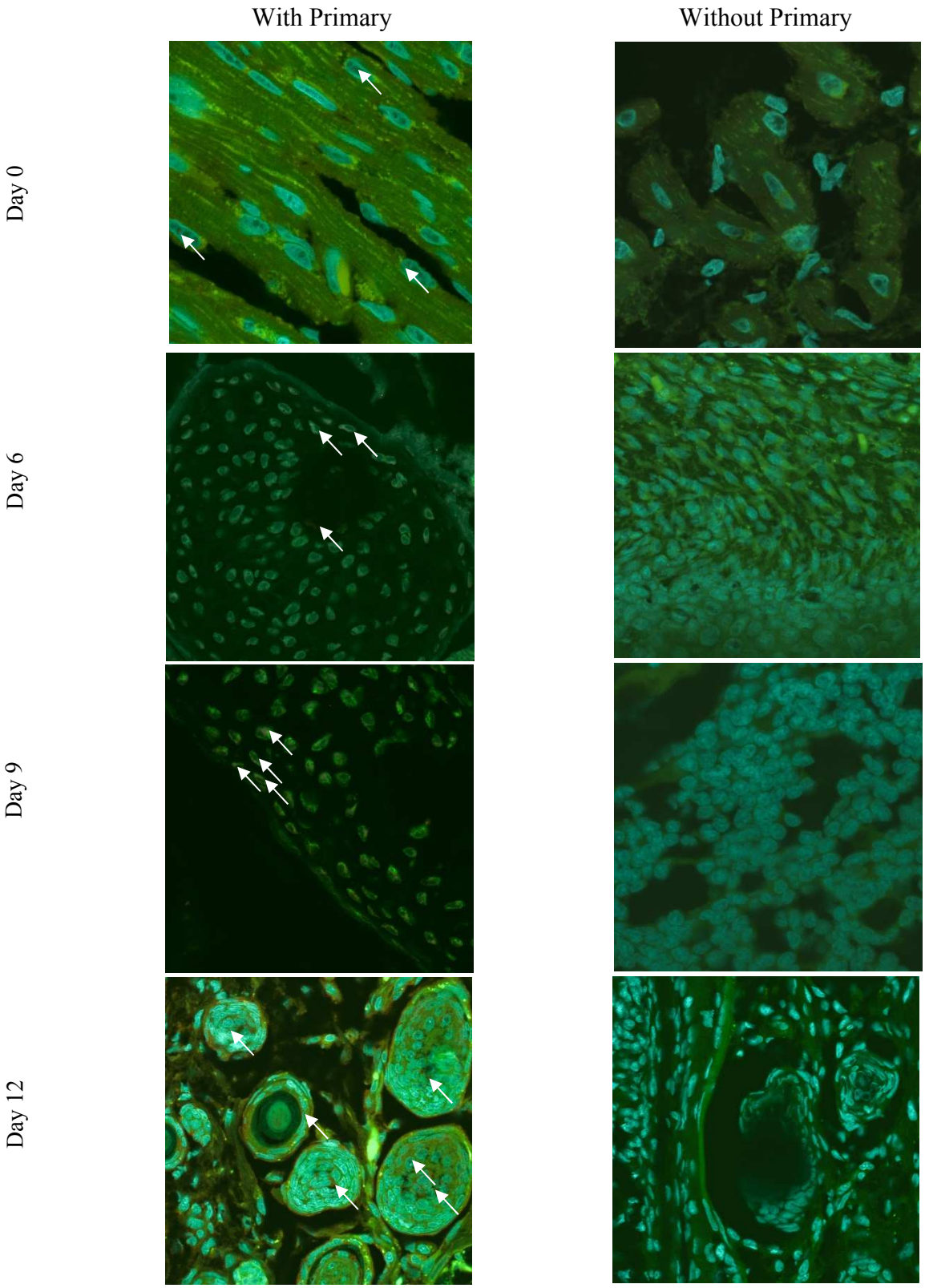

Figure 2. Confirmation of NS1 Protein in Infected Pups. White arrows show nuclei displaying signs of ZIKV infection (red). Sections stained with anti-ZIKV NS1 monoclonal antibody (red). Cytoskeleton is stained green; nuclei are blue. Day 3 was omitted due to no observed infection.

Dams Evaluated				Pups Evaluated		NS1 Score	
ID	Route	Sex	Treatment	ID	Age (Days)	Head	Body
1341	IP	F	ZIKV-BR	-	-	-	-
1349	IM	F	ZIKV-BR	P1349-11	9	*	1
				P1349-12	9	1	1
1350	IM	F	ZIKV-BR	-	-	-	-
1351	IM	F	ZIKV-BR	-	-	-	-
1366	IM	F	ZIKV-BR	-	-	-	-
1397	SC	F	ZIKV-BR	-	-	-	-
1424	IM	F	ZIKV-BR	-	-	-	-
1426	SC	F	ZIKV-BR	-	-	-	-
1465	IM	F	ZIKV-BR	-	-	-	-
1475	IP	F	ZIKV-BR	-	-	-	-
1477	IP	F	ZIKV-BR	-	-	-	-
1493	SC	F	ZIKV-BR	-	-	-	-
1330	IP	F	PBS	-	-	-	-
1521	IP	F	PBS	-	-	-	-
1540	IP	F	PBS	-	-	-	-
1541	IP	F	PBS	P1541-9	3	0	0
1542	IM	F	PBS	-	-	-	-
1545	SC	F	PBS	-	-	-	-

Table 2: Evaluation of Dams and Pups. The table illustrates the ID numbers of the Dams of these pups that were evaluated and tested for ZIKV-BR. Of the total pups tested, three pups were found to correlate with the dams tested and their corresponding NS1 score is listed. *; tissue was fixed and sectioned but not stained due to time constraints.

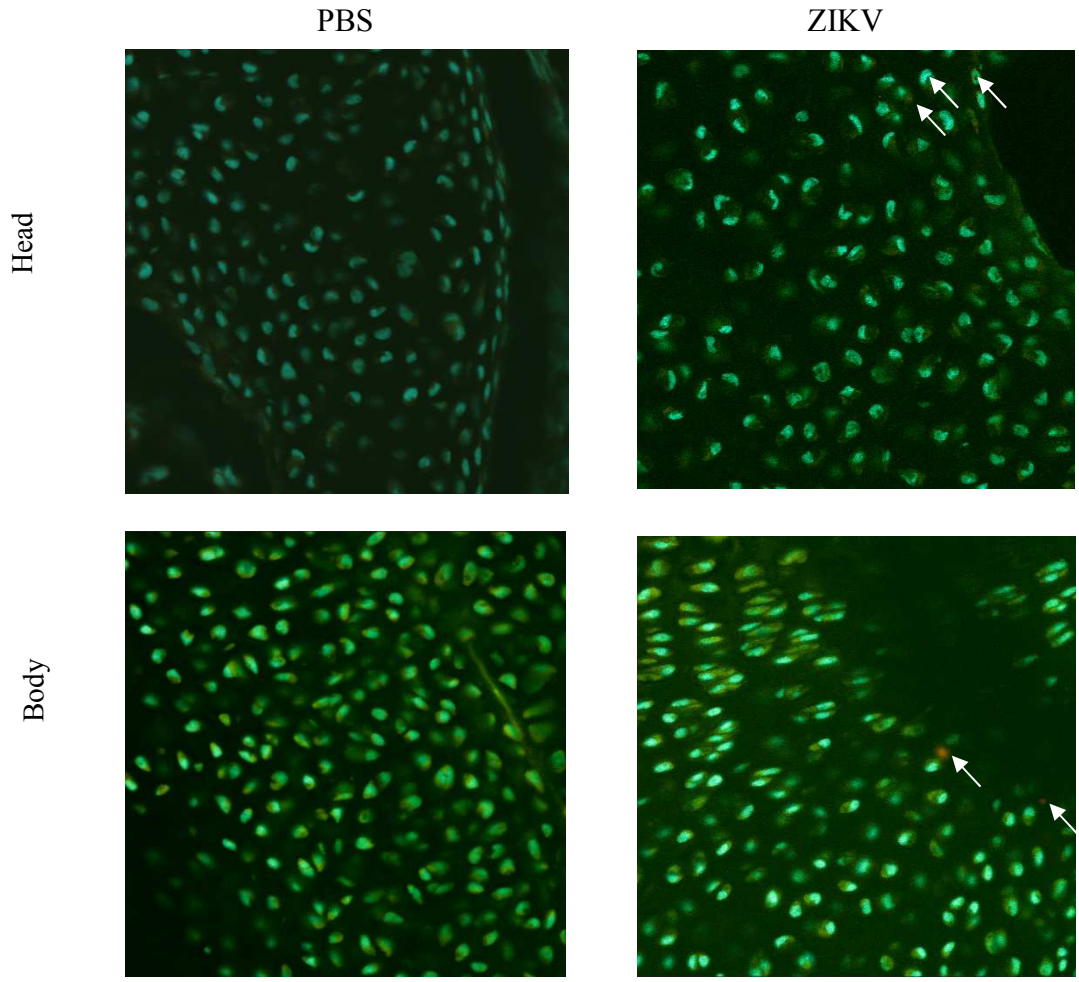

Figure 3. Comparisons of PBS-Treated and ZIKV Pups. White arrows illustrate ZIKV infection (red).

Total Heads Evaluated	Total Heads Infected	Percentage Infected (Heads only)
16	10	63%
Total Bodies Evaluated	Total Bodies Infected	Percentage Infected (Bodies only)
13	10	77%
Total Tissues Evaluated (Both Heads and Bodies)	Total Tissues Infected	Total Percentage Infected
29	20	69%

Table 3. Percentage of Infection in Tissues. The table shows the whether the heads, bodies, or heads and bodies were infected. The PBS group was omitted in the percentage infected as they were the control.

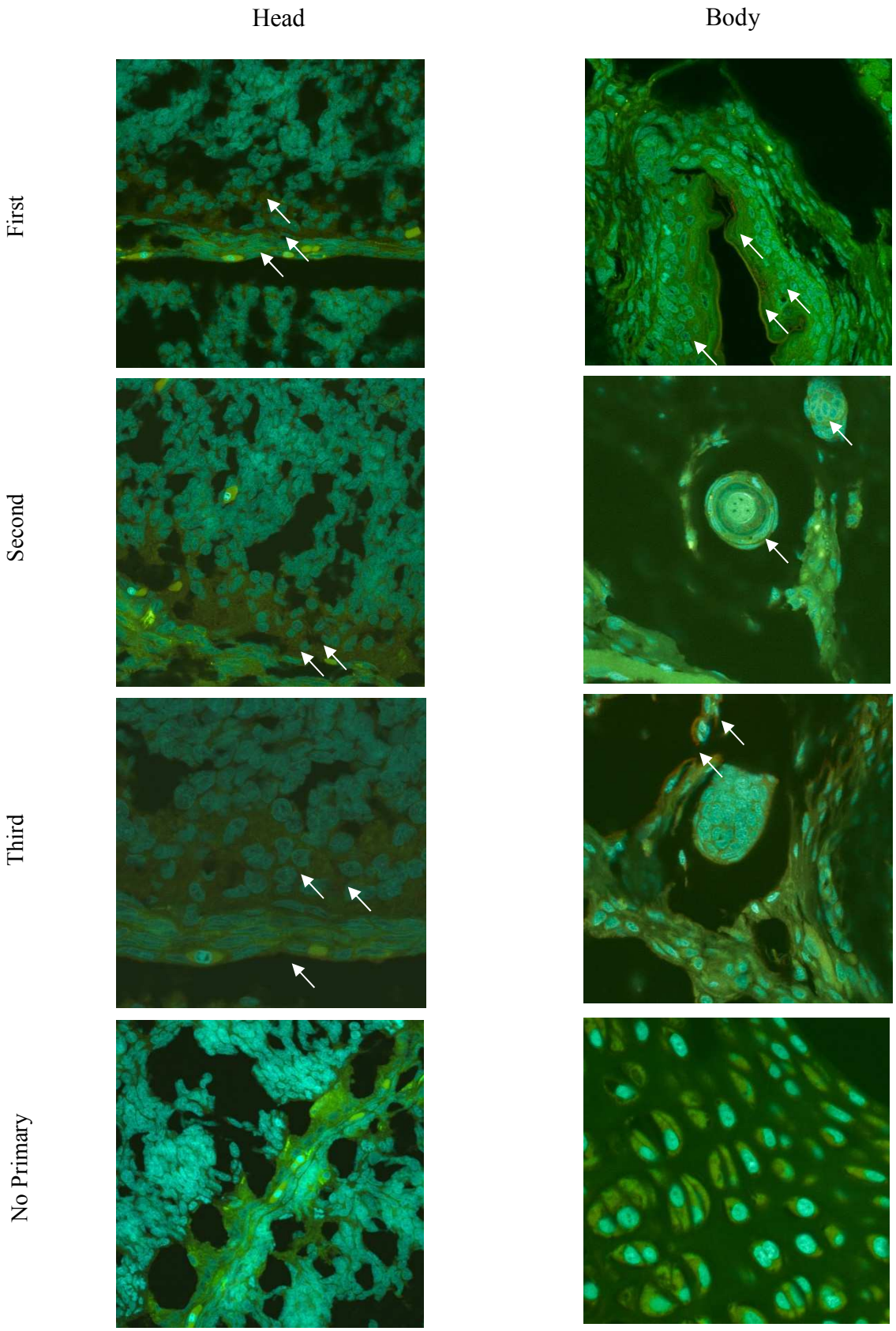

Figure 4: Triplicates of IHC. The images illustrate how stained images are done in triplicates. Both the head and body are done in triplicates to show consistent infection in certain areas. A no primary image was added to each corresponding triplicate.

TISSUES EVALUATED	TOTAL TISSUES INFECTED	AGE (DAYS)	PERCENTAGE INFECTED
2	2	0	100%
4	0	3	0%
6	3	6	50%
7	5	9	71%
10	10	12	100%

Table 4: Percentage of Infection based on Age. The table reveals the observed infection rate of each pup age relative to the tissues evaluated in that age group. PBS group was omitted in the calculation of percentage infected as they were the control.

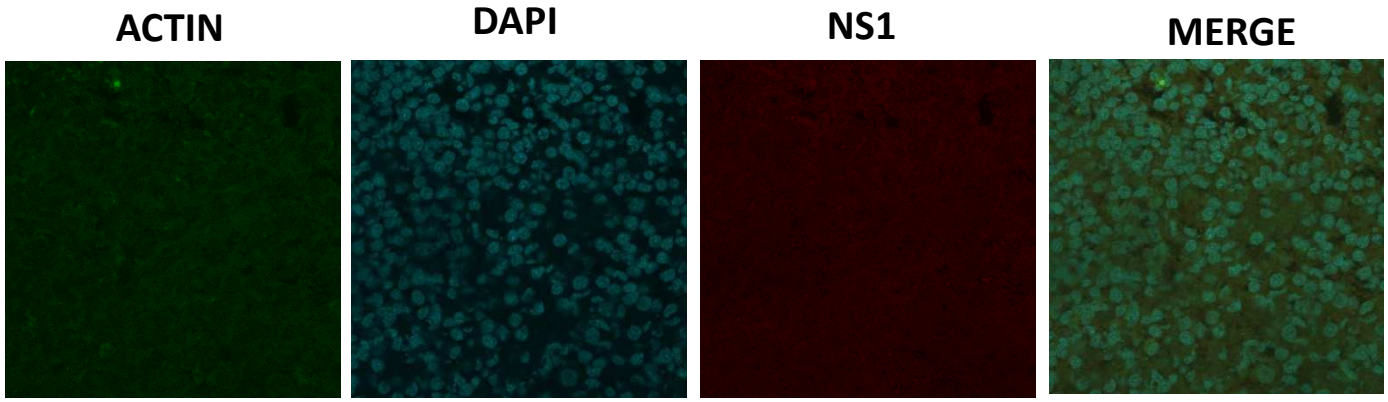

Figure 5. Various channels for Confocal Microscopy. The figure above illustrates the various channels of ACTIN, DAPI, NS1, and MERGE in a Day 12 opossum pup.

Group #	ID Number	Age (days)	Treatment	NS1 Score (Head, Body)		Additional Comments
				Head	Body	
3	P1349-12	9d	B	1	1	Frozen
	P1349-11	9d	B	*	1	Formalin Fixed
	P1359-9	9d	B	0	*	Frozen
	P1364-11	9d	B	3	1	Frozen
5	P1398-9	6d	B	1	1	Frozen
	P1398-8	6d	B	0	0	Formalin Fixed
6	P1455-9	12d	B	1	*	Formalin Fixed
	P1467-10	12d	B	1	1	Formalin Fixed
	P1467-9	12d	B	1	1	Frozen
7	P1494-9	0d	B	*	*	Formalin Fixed
	P1476-9	0d	B	1	1	Formalin Fixed
	P1495-10	9d	B	0	*	Frozen
	P1495-8	12d	B	3	*	Formalin Fixed
8	P1504-8	12d	PBS	*	2	Frozen
9	P1520-11	3d	PBS	0	0	Frozen
10	P1541-9	3d	PBS	0	0	Frozen
11	P1569-9	6d	B	0	1	Frozen
	P1584-8	12d	B	2	*	Formalin Fixed
	P1591-10	12d	B	2	1	Formalin Fixed

Table 5: Pups and Corresponding litters. The table above depicts the individual pups born from mothers of their respective groups. NS1 scores are the same from Table 1; *, illustrates a tissue that has not been stained.

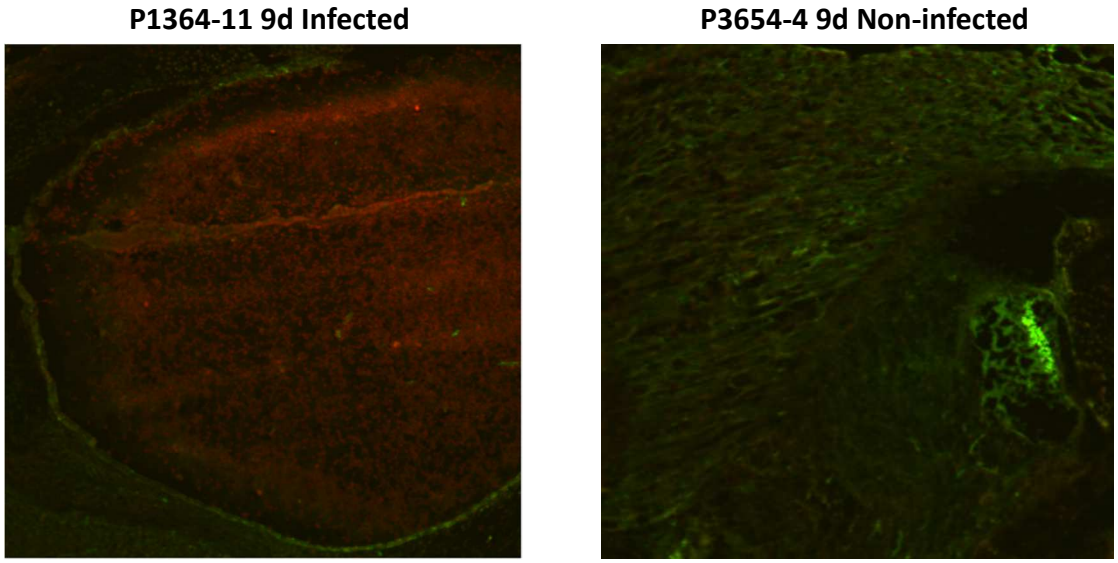

Figure 6: Apoptosis Assay of Day 9 pup. The figure above depicts an apoptosis assay done on an infected Day 9 pup and a PBS control pup. Images are taken at 10x magnification of the brain. Red depicts apoptosis; green depicts the cytoskeleton.

REFERENCES

Adams Waldorf K.M., Stencel-Baerenwald J.E., Kapur R.P., Studholme C., Boldenow E., Vornhagen J., Baldessari A., Dighe M.K., Thiel J., Merillat S., et al. Fetal brain lesions after subcutaneous inoculation of Zika virus in a pregnant nonhuman primate. Nat. Med. 2016;22:1256–1259. doi: 10.1038/nm.4193.

Aid, M., Abbink, P., Larocca, R. A., Boyd, M., Nityanandam, R., Nanayakkara, O., et al. (2017). Zika virus persistence in the central nervous system and lymph nodes of rhesus monkeys. Cell 169, 610.e14–620.e14. doi: 10.1016/j.cell.2017.04.008

Avirutnan, P. et al. Secreted NS1 of dengue virus attaches to the surface of cells via interactions with heparan sulfate and chondroitin sulfate E. PLoS Pathog. 3, e183 (2007).

Bayer A, Lennemann NJ, Ouyang Y, Bramley JC, Morosky S, Marques ET Jr, Cherry S, Sadovsky Y, Coyne CB (2016) Type interferons produced by human placental trophoblasts confer protection against Zika virus infection. Cell Host Microbe 19:705–712. doi: 10.1016/j.chom.2016.03.008

Brasil P, Pereira JP, Jr., Moreira ME, Ribeiro Nogueira RM, Damasceno L, Wakimoto M, Rabello RS, Valderramos SG, Halai UA, Salles TS, Zin AA, Horovitz D, Daltro P, Boechat M, Raja Gabaglia C, Carvalho de Sequeira P, Pilotto JH, Medialdea-Carrera R, Cotrim da Cunha D, Abreu de Carvalho LM, Pone M, Machado Siqueira A, Calvet GA, Rodrigues Baiao AE, Neves ES, Nassar de Carvalho PR, Hasue RH, Marschik PB, Einspieler C, Janzen C, Cherry JD, Bispo de Filippis AM, Nielsen-Saines K. 2016. Zika virus infection in pregnant women in Rio de Janeiro. N Engl J Med 375(24):2321–2334.

Bueno M.G., Martinez N., Abdalla L., dos Santos C.N.D., Chame M. Animals in the Zika Virus Life Cycle: What to Expect from Megadiverse Latin American Countries. PLoS Neglect. Trop. Dis. 2016;10:e0005073. doi: 10.1371/journal.pntd.0005073

Caine, Elizabeth, et al. “Animal Models of Zika Virus Infection During Pregnancy.” Viruses 10.11 (2018): 598–.

Calvet, G., Aguiar, R. S., Melo, A. S., Sampaio, S. A., de Filippis, I., Fabri, A., et al. (2016).

Detection and sequencing of Zika virus from amniotic fluid of fetuses with microcephaly in Brazil: a case study. Lancet Infect. Dis. 16, 253–260. doi: 10.1016/S1473-3099(16)00095-5.

Cao B., Parnell L.A., Diamond M.S., Mysorekar I.U. Inhibition of autophagy limits vertical transmission of Zika virus in pregnant mice. J. Exp. Med. 2017;214:2303–2313. doi: 10.1084/jem.20170957.

Cardoso-Moreira, Margarida, et al. "Gene Expression Across Mammalian Organ Development." *Nature (London)* 571.7766 (2019): 505–509.

Cauchemez S, Besnard M, Bompard P, Dub T, Guillemette-Artur P, Eyrolle-Guignot D, Salje H, Van Kerkhove MD, Abadie V, Garel C, Fontanet A, Mallet HP. 2016. Association between Zika virus and microcephaly in French Polynesia, 2013–2015: a retrospective study. Lancet 387(10033):2125–2132.

Colt, S., Garcia-Casal, M., Peña-Rosas, J., Finkelstein, J., Rayco-Solon, P., Weise Prinzo, Z., et al. (2017). Transmission of Zika virus through breast milk and other breastfeeding-related bodily-fluids: a systematic review. PLOS Negl. Trop. Dis. 11:e0005528. doi: 10.1371/journal.pntd.0005528

Devika Sirohi, Richard J Kuhn, Zika Virus Structure, Maturation, and Receptors, The Journal of Infectious Diseases, Volume 216, Issue suppl_10, 15 December 2017, Pages S935–S944, https://doi.org/10.1093/infdis/jix515.

Dowall SD, Graham VA, Rayner E, Atkinson B, Hall G, Watson RJ, Bosworth A, Bonney LC, Kitchen S, Hewson R (2016) A susceptible mouse model for Zika virus infection. PLoS Negl Trop Dis 10:e0004658. doi: 10.1371/journal.pntd.0004658.

Dudley DM, Aliota MT, Mohr EL, Weiler AM, Lehrer-Brey G, Weisgrau KL, Mohns MS, Breitbach ME, Rasheed MN, Newman CM, Gellerup DD (2016) A rhesus macaque model of Asian-lineage Zika virus infection. Nat Commun 7:12204. doi: 10.1038/ncomms12204

Elshahawi, H., Syed Hassan, S., & Balasubramaniam, V. (2019). Importance of Zika Virus NS5 Protein for Viral Replication. Pathogens (Basel, Switzerland), 8(4), 169. https://doi.org/10.3390/pathogens8040169.

Goodfellow FT, Tesla B, Simchick G, Zhao Q, Hodge T, Brindley MA, Stice SL (2016) Zika virus induced mortality and microcephaly in chicken embryos. Stem Cells Dev 25:1691–1697. doi: 10.1089/scd.2016.0231.

Grant A, Ponia SS, Tripathi S, Balasubramaniam V, Miorin L, Sourisseau M, Schwarz MC, Sanchez-Seco MP, Evans MJ, Best SM, Garcia-Sastre A. 2016. Zika virus targets human STAT2 to inhibit type I interferon signaling. Cell Host Microbe 19(6):882–890.

Grant, A., Ponia, S. S., Tripathi, S., Balasubramaniam, V., Miorin, L., Sourisseau, M., et al. (2016). Zika virus targets human STAT2 to inhibit type I interferon signaling. Cell Host Microbe 19, 882–890. doi: 10.1016/j.chom.2016.05.009.

Honein M.A., Dawson A.L., Petersen E.E., Jones A.M., Lee E.H., Yazdy M.M., Ahmad N., Macdonald J., Evert N., Bingham A., et al. Birth Defects Among Fetuses and Infants of US Women With Evidence of Possible Zika Virus Infection During Pregnancy. JAMA. 2017;317:59–68. doi: 10.1001/jama.2016.19006.

Infante, A.J., Samples, N.K., Croix, D.A., Redding, T.S. Cellular Immune Response of a Marsupial, *Monodelphis domestica*. Developmental and Comparative Immunology, 15:1, 189-1999.

Jampol L.M., Goldstein D.A. Zika Virus Infection and the Eye. JAMA Ophthalmol. 2016;134:535–536. doi: 10.1001/jamaophthalmol.2016.0284

Jennifer L Spencer, Anismrita Lahon, Linda L Tran, Ravi P Arya, Alexander R Kneubehl, Megan B Vogt, Daniela Xavier, David R Rowley, Jason T Kimata, Rebecca R Rico-Hesse, Replication of Zika Virus in Human Prostate Cells: A Potential Source of Sexually Transmitted Virus, The Journal of Infectious Diseases, Volume 217, Issue 4, 15 February 2018, Pages 538–547, https://doi.org/10.1093/infdis/jix436.

Kammerer, C.M., Rainwater, D.L., Gouin, N., Jasti, M. et al., 2010. Localization of genes for V+LDL plasma cholesterol levels on two diets in the opossum *Monodelphis domestica*. October 2010, Journal of Lipid Research. 51, 2929-2939.

Kuhn, R.J., 2015. Understanding Zika virus structure and replication. NAS and IOM Zika Virus Workshop, Feb 16, 2015.

Kumar, A., Hou, S., Airo, A. M., Limonta, D., Mancinelli, V., Branton, W., et al. (2016). Zika virus inhibits type-I interferon production and downstream signaling. EMBO Rep. 17, 1766–1775. doi: 10.15252/embr.201642627

Kushwaha, R., & VandeBerg, J. (2004). Effect of dietary cholesterol with or without saturated fat on plasma lipoprotein cholesterol levels in the laboratory opossum (Monodelphis domestica) model for diet-induced hyperlipidaemia. British Journal of Nutrition, 92(1), 63-70. doi:10.1079/BJN20041167

Lazear HM, Govero J, Smith AM, Platt DJ, Fernandez E, Miner JJ, Diamond MS. 2016. A mouse model of Zika virus pathogenesis. Cell Host Microbe 19(5):720–730

Ley, R.D., 2007. Dose Response for Ultraviolet Radiation A–induced Focal Melanocytic Hyperplasia and Nonmelanoma Skin Tumors in *Monodelphis domestica*. Photochemistry & Photobiology Jan 2001 73:1, 20-23. https://doi.org/10.1562/0031-8655(2001)0730020DRFURA2.0.CO2.

Ley, R.D., Applegate, L.A., 1985. Ultraviolet Radiation-Induced Histopathologic Changes in the Skin of the Marsupial Monodelphis domestica II. Quantitative Studies of the Photoreactivation of Induced Hyperplasia and Sunburn Cell Formation. Inv Derma October 1985 85:4, 365-367. https://doi.org/10.1111/1523-1747.ep12276992

Li, G., Poulsen, M., Fenyvuesvolgyi, C., Yashiroda, Y., Yoshida, M., Simard, J. M., et al. (2017). Characterization of cytopathic factors through genome-wide analysis of the Zika viral proteins in fission yeast. Proc. Natl. Acad. Sci. U.S.A. 114, E376–E385. doi: 10.1073/pnas.1619735114.

Lucchese, G., and Kanduc, D. (2016). Zika virus and autoimmunity: from microcephaly to Guillain-Barre syndrome, and beyond. Autoimmun. Rev. 15, 801–808. doi: 10.1016/j.autrev.2016.03.020

Magnani D.M., Rogers T.F., Maness N.J., Grubaugh N.D., Beutler N., Bailey V.K., Gonzalez-Nieto L., Gutman M.J., Pedreno-Lopez N., Kwal J.M., et al. Fetal demise and failed antibody therapy during Zika virus infection of pregnant macaques. Nat. Commun. 2018;9:1624. doi: 10.1038/s41467-018-04056-4.

Manangeeswaran M, Ireland DD, Verthelyi D (2016) Zika (PRVABC59) infection is associated with T cell infiltration and neurodegeneration in CNS of immunocompetent neonatal C57Bl/6 mice. PLoS Pathog 12:e1006004

Meaney-Delman, D., Hills, S. L., Williams, C., Galang, R. R., Iyengar, P., Hennenfent, A. K., et al. (2016). Zika virus infection among U.S. pregnant travelers – August 2015–February 2016. MMWR Morb. Mortal. Wkly. Rep. 65, 211–214. doi: 10.15585/mmwr.mm6508e1

Miner JJ, Cao B, Govero J, Smith AM, Fernandez E, Cabrera OH, Garber C, Noll M, Klein RS, Noguchi KK, Mysorekar IU (2016) Zika virus infection during pregnancy in mice causes placental damage and fetal demise. Cell 165:1081–1091. doi: 10.1016/j.cell.2016.05.008

Monel, B., Compton, A. A., Bruel, T., Amraoui, S., Burlaud-Gaillard, J., Roy, N., et al. (2017). Zika virus induces massive cytoplasmic vacuolization and paraptosis-like death in infected cells. EMBO J. 36, 1653–1668. doi: 10.15252/embj.201695597

Monsalve, D. M., Pacheco, Y., Acosta-Ampudia, Y., Rodríguez, Y., Ramírez-Santana, C., and Anaya, J.-M. (2017). Zika virus and autoimmunity. One-step forward. Autoimmun. Rev. 16, 1237–1245. doi: 10.1016/j.autrev.2017.10.008.

Mostegl, Meike M., et al. "Influence of Prolonged Formalin Fixation of Tissue Samples on the Sensitivity of Chromogenic in Situ Hybridization." Journal of Veterinary Diagnostic Investigation 23.6 (2011): 1212–1216

Morrison TE, Diamond MS. 2017. Animal models of Zika virus infection, pathogenesis, and immunity. J Virol 91:e00009-17. https://doi.org/10.1128/JVI.00009-17.

Muñoz, L. S., Barreras, P., and Pardo, C. A. (2016). Zika Virus-associated neurological disease in the adult: guillain-barre syndrome, Encephalitis, and Myelitis. Semin. Reprod. Med. 34, 273–279. doi: 10.1055/s-0036-1592066.

Musso, D., Nilles, E. J., and Cao-Lormeau, V.-M. (2014). Rapid spread of emerging Zika virus in the Pacific area. *Clin. Microbiol. Infect.* 20, O595–O596. doi: 10.1111/1469-0691.12707

Mysorekar IU, Diamond MS. 2016. Modeling Zika virus infection in pregnancy. N Engl J Med 375:481– 484. https://doi.org/10.1056/NEJMcibr1605445.

Nem de Oliveira Souza, Isis, et al. "Acute and Chronic Neurological Consequences of Early-Life Zika Virus Infection in Mice." Science translational medicine 10.444 (2018): eaar2749–.

Oshiumi, H., Kouwaki, T., and Seya, T. (2016). Accessory factors of cytoplasmic viral rna sensors required for antiviral innate immune response. Front. Immunol. 7:200. doi: 10.3389/fimmu.2016.00200.

Pagani, I., Ghezzi, S., Ulisse, A., Rubio, A., Turrini, F., Garavaglia, E., et al. (2017). Human endometrial stromal cells are highly permissive to productive infection by Zika virus. Sci. Rep. 7:44286. doi: 10.1038/srep44286.

Parameswaran P, Sklan E, Wilkins C, Burgon T, Samuel MA, Lu R, Ansel KM, Heissmeyer V, Einav S, Jackson W, Doukas T, Paranjape S, Polacek C, dos Santos FB, Jalili R, Babrzadeh F, Gharizadeh B, Grimm D, Kay M, Koike S, Sarnow P, Ronaghi M, Ding

SW, Harris E, Chow M, Diamond MS, Kirkegaard K, Glenn JS, Fire AZ. 2010. Six RNA viruses and forty-one hosts: viral small RNAs and modulation of small RNA repertoires in vertebrate and invertebrate systems. PLoS Pathog 6(2):e1000764.

Potisopon S., Priet S., Collet A., Decroly E., Canard B., Selisko B. The methyltransferase domain of dengue virus protein NS5 ensures efficient RNA synthesis initiation and elongation by the polymerase domain. Nucleic Acids Res. 2014;42:11642–11656. doi: 10.1093/nar/gku666.

Qian X, Nguyen HN, Song MM, Hadiono C, Ogden SC, Hammack C, Yao B, Hamersky GR, Jacob F, Zhong C, Yoon KJ (2016) Brainregion-specific organoids using mini-bioreactors for modeling ZIKV exposure. Cell 165:1238–1254. doi: 10.1016/j.cell.2016.04.032.

Rather IA, Lone JB, Bajpai VK, Paek WK and Lim J (2017). Zika Virus: An Emerging Worldwide Threat. Front. Microbiol. 8:1417. doi: 10.3389/fmicb.2017.01417.

Roby, J. A., Setoh, Y. X., Hall, R. A., and Khromykh, A. A. (2015). Post-translational regulation and modifications of flavivirus structural proteins. J. Gen. Virol. 96, 1551–1569. doi: 10.1099/vir.0.000097.

Rodriguez, A. K., Muñoz, A. L., Segura, N. A., Rangel, H. R., & Bello, F. (2019). Molecular characteristics and replication mechanism of dengue, zika and chikungunya arboviruses, and their treatments with natural extracts from plants: An updated review. EXCLI journal, 18, 988–1006. https://doi.org/10.17179/excli2019-1825

Ronald D. Ley, Lee A. Applegate, R. J. Michael Fry and Anne B. Sanchez. Photoreactivation of Ultraviolet Radiation-induced Skin and Eye Tumors of *Monodelphis domestica*. Cancer Res December 15 1991 (51) (24) 6539-6542.

Rossi SL, Tesh RB, Azar SR, Muruato AE, Hanley KA, Auguste AJ, Langsjoen RM, Paessler S, Vasilakis N, Weaver SC. 2016. Characterization of a novel murine model to study Zika virus. Am J Trop Med Hyg 94:1362–1369. https://doi.org/10.4269/ajtmh.16-0111.

Sarno M, Sacramento GA, Khouri R, do Rosário MS, Costa F, Archanjo G, Santos LA, Nery N, Jr, Vasilakis N, Ko AI, de Almeida AR. 2016. Zika virus infection and stillbirths: a case of hydrops fetalis, hydranencephaly and fetal demise. PLoS Negl Trop Dis 10(2):e0004517.

Savidis, G., Perreira, J. M., Portmann, J. M., Meraner, P., Guo, Z., Green, S., et al. (2016). The IFITMs Inhibit Zika Virus Replication. Cell Rep. 15, 2323–2330. doi:

10.1016/j.celrep.2016.05.074

Sejvar, J. J., Baughman, A. L., Wise, M., and Morgan, O. W. (2011). Population incidence of Guillain-Barre syndrome: a systematic review and meta-analysis. Neuroepidemiology 36, 123–133. doi: 10.1159/000324710

Smith DR, Hollidge B, Daye S, Zeng X, Blancett C, Kuszpit K, Bocan T, Koehler JW, Coyne S, Minogue T, Kenny T (2017) Neuropathogenesis of Zika virus in a highly susceptible immunocompetent mouse model after antibody blockade of type interferon. PLoS Negl Trop Dis 11:e0005296. doi: 10.1371/journal.pntd.0005296.

Tang H, Hammack C, Ogden SC, Wen Z, Qian X, Li Y, Yao B, Shin J, Zhang F, Lee EM, Christian KM (2016) Zika virus infects human cortical neural progenitors and attenuates their growth. Cell Stem Cell 18:587–590. doi: 10.1016/j.stem.2016.02.016.

VandeBerg, J.L. and Williams-Blangero S. "The Laboratory Opossum." The UFAW Handbook on the Care and Management of Laboratory and Other Research Animals. (2010): Jan 19;8:246-61

van den Pol, Anthony N., et al. "Zika Virus Targeting in the Developing Brain." The Journal of neuroscience 37.8 (2017): 2161–2175.

Venturi G., Zammarchi L., Fortuna C., Remoli M.E., Benedetti E., Fiorentini C., Trotta M., Rizzo C., Mantella A., Rezza G., et al. An autochthonous case of Zika due to possible sexual transmission, Florence, Italy, 2014. Eurosurveillance. 2016;21:2–5. doi: 10.2807/1560-7917.ES.2016.21.8.30148.

Weaver, S. C., Costa, F., Garcia-Blanco, M. A., Ko, A. I., Ribeiro, G. S., Saade, G., et al. (2016). Zika virus: history, emergence, biology, and prospects for control. Antiviral Res. 130, 69–80. doi: 10.1016/j.antiviral.2016.03.010

Yockey LJ, Varela L, Rakib T, Khoury-Hanold W, Fink SL, Stutz B, Szigeti-Buck K, Van den Pol A, Lindenbach BD, Horvath TL, Iwasaki A (2016) Vaginal exposure to Zika virus during pregnancy leads to fetal brain infection. Cell 166:1247–1256.e4 doi: 10.1016/j.cell.2016.08.004.

Young, Paul R et al. "An Antigen Capture Enzyme-Linked Immunosorbent Assay Reveals High Levels of the Dengue Virus Protein NS1 in the Sera of Infected Patients." *Journal of clinical microbiology* 38.3 (2000): 1053–1057.

Yun, S.-I., Song, B.-H., Frank, J. C., Julander, J. G., Polejaeva, I. A., Davies, C. J., et al. (2016).

Complete genome sequences of three historically important, spatiotemporally distinct, and genetically divergent strains of Zika virus: MR-766, P6-740, and PRVABC-59. Genome Announc. 4:e00800-16. doi: 10.1128/genomeA.00800-16.

Zhao B., Yi G., Du F., Chuang Y.-C., Vaughan R.C., Sankaran B., Kao C.C., Li P. Structure and function of the Zika virus full-length NS5 protein. Nat. Commun. 2017;8:14762. doi: 10.1038/ncomms14762.

Zhao, L., Alto, B. W., Smartt, C. T., and Shin, D. (2018). Transcription profiling for defensins of Aedes aegypti (Diptera: Culicidae) during development and in response to infection with Chikungunya and Zika viruses. J. Med. Entomol. 55, 78–89. doi: 10.1093/jme/tjx174

Zmurko J, Marques RE, Schols D, Verbeken E, Kaptein SJ, Neyts J (2016) The viral polymerase inhibitor 7-deaza-20-C-methyladenosine is a potent inhibitor of in vitro Zika virus replication and delays disease progression in a robust mouse infection model. PLoS Negl Trop Dis 10:e0004695. doi: 10.1371/journal.pntd.0004695.

BIOGRAPHICAL SKETCH

Dionn Carlo Silva earned his Master of Science degree in Biochemistry and Molecular Biology at the University of Texas Rio Grande Valley in 2021, where he focused on the vertical transmission of Zika virus in the laboratory opossum. In December of 2018, Dionn Carlo received his Bachelor of Science degree in Biology from UTRGV. During his time at UTRGV, Dionn Carlo also participated in the processing and testing of patient samples for COVID-19 under the direction of Dr. John Thomas. Dionn Carlo's research interests include virology, immunology, and microbiology. Dionn Carlo wants to pursue an M.D. Ph D. and has an interest in infectious diseases. He can reached at dionncarlo@gmail.com .